The Journal of Chemical Physics

The excitonic effects in single and double-walled boron nitride nanotubes

Cite as: J. Chem. Phys. **140**, 244701 (2014); https://doi.org/10.1063/1.4880726
Submitted: 20 January 2014 . Accepted: 19 May 2014 . Published Online: 23 June 2014

Shudong Wang, Yunhai Li, Joanne Yip, and Jinlan Wang

The excitonic effects in single and double-walled boron nitride nanotubes

Shudong Wang,[1] Yunhai Li,[1] Joanne Yip,[2] and Jinlan Wang[1,a)]
[1]*Department of Physics and Key Laboratory of MEMS of Ministry of Education, Southeast University, Nanjing 211189, China*
[2]*Institute of Textiles and Clothing, Hong Kong Polytechnic University, Kowloon, Hong Kong, China*

(Received 20 January 2014; accepted 19 May 2014; published online 23 June 2014)

The electronic structures and excitonic optical properties of single- and double-walled armchair boron nitride nanotubes (BNNTs) [e.g., (5,5) and (10,10), and (5,5)@(10,10)] are investigated within many-body Green's function and Bethe-Salpeter equation formalism. The first absorption peak of the double-walled nanotube has almost no shift compared with the single-walled (5,5) tube due to the strong optical transition in the double-walled tube that occurs within the inner (5,5) one. Dark and semi-dark excitonic states are detected in the lower energy region, stemming from the charge transfer between inner and outer tubes in the double-walled structure. Most interestingly, the charge transfer makes the electron and the hole reside in different tubes. Moreover, the excited electrons in the double-walled BNNT are able to transfer from the outer tube to the inner one, opposite to that which has been observed in double-walled carbon nanotubes. © *2014 AIP Publishing LLC*. [http://dx.doi.org/10.1063/1.4880726]

I. INTRODUCTION

Since the discovery of carbon nanotubes (CNTs),[1] boron nitride nanotubes (BNNTs), including both single-walled[2,3] and multi-walled[4,5] nanotubes, whose structures are analogous to CNTs, have also been fabricated successfully.[4–6] Unlike CNTs, whose gaps are dependent on the diameter and chirality of the tubes, the mechanical stability, chemical inertia, and electronic insulating properties of BNNTs with diameters larger than 9.5 Å are insensitive to the diameter and the chirality.[7,8] The optical properties, which depend strongly on the band gaps, play a crucial role in nano-optoelectronic devices and structure characterization of BNNTs.[9,10] Theoretical[11,12] and experimental[13–15] studies have shown that excitonic effects dramatically alter the optical properties in single-walled BNNTs and they are very distinct due to the wide band gap of BNNTs.[9,16–22] For example, Wirtz *et al.*[16] and Park *et al.*[17] found that there are bound excitonic peaks in single-walled BNNTs. The strong excitonic effects of BNNTs make them compelling candidates for field-effect transistors[23] and ultraviolet light sources.[24,25]

In BNNTs, due to the strong ionicity of B–N bonds, double- or multi-walled BNNT structures are easy to form and most of the synthesized multi-walled BNNTs are even walls.[26,27] For typical multi-walled BNNTs, the distances between the walls are about 3.3-3.5 Å,[28,29] close to that of the neighboring layers in hexagonal BN bulk. For the simplest multi-walled BNNTs, double-walled BNNTs, the highest valence band and the lowest conduction band are localized at the outer and the inner tubes, respectively,[28,30] stemming from the hybridization between the σ states and π states of both tubes induced by the large curvature of the tubes. This unique electronic structure makes the double-walled BNNTs as type II semiconducting hetero-structure, in which conduction bands and valence bands reside in different substructures. In this situation, when the system is excited by light, the excited electrons and holes may reside in two different tubes and the resultant excitons are thus different from those in single-walled BNNTs. Actually, the separation of electrons and holes and location in different tubes were observed experimentally[31–33] in double-walled CNTs.

For double or multi-walled BNNTs with diameters of 15-30 Å, their optical gaps are about 5.8 ± 0.2 eV, close to the value of bulk *h*-BN.[10] Jaffrennou and co-workers[22,34] have investigated multi-walled BNNTs with diameters of 30-150 nm and found that the ultraviolet emission resulted from the exciton recombination, and the exciton bands were red-shift compared to *h*-BN bulk. These studies on multi-walled BNNTs involve neither the exciton transfer between tubes nor the optical absorption property related to the exciton transfer. Besides, most of theoretical studies focus on single-walled BNNTs. Therefore, it is very necessary to study the optical properties, especially including the exciton effect, of multi-walled BNNTs. In this article, we take a double-walled armchair BNNT (5,5)@(10,10) as an example to investigate the electronic structures and optical absorption properties and compare them with their component single-walled BNNTs via *GW* approximation and Bethe-Salpeter equation (BSE). The first absorption peak of the double-walled nanotube is exactly the same as that of the single-walled (5,5) tube stemming from the fact that the strongest optical transition in the double-walled tube occurs within the inner (5,5) one. Dark or semi-dark excitons are found in double-walled BNNTs, and they are related to the electron transfer between tubes. These charge transfer induced excitons make electrons and holes reside in different tubes in double-walled structures, just as the type-II semiconducting hetero-structure, which can effectively separate electrons and holes. The exciton binding energies in double-walled BNNTs are lower than their counterparts in single-walled ones as well.

a)Electronic mail: jlwang@seu.edu.cn.

II. COMPUTATIONAL METHOD

We take three steps to calculate the quasiparticle energy and optical properties.[35] First, we use the Quantum-ESPRESSO package[36] to obtain the ground state and electronic band structures. Local density approximation (LDA) is adopted and the kinetic cutoff of 45 Ry is used. The 15 Å vacuum is taken to avoid the interactions among neighboring tubes. Each atomic structure is fully relaxed until forces acting on each atom are less than 1×10^{-2} eV/Å. The Brillouin zone integration is done by $1 \times 1 \times 21$ k-point sampling within the Monkhorst-Pack scheme. Next, the quasiparticle energies are calculated through GW approximation.[37,38] The plasmon-pole approximation[39,40] is used to calculate the screened Coulomb interaction W. 460 (500) empty bands, 4 Ry and 50 Ry energy cutoff are taken to obtain the dielectric matrices and self-energy in single-walled BNNT (5,5), respectively. Finally, the electron-hole interaction is considered via solving the Bethe-Salpeter equation.[41,42] We take 10 valence bands and 15 conduction bands to obtain the optical absorption spectra. For calculating the static screening in W, 50 Ry and 4 Ry are used for exchange and attraction matrices in single-walled BNNT (5,5), respectively. A box-shape truncated Coulomb interaction is used to simulate truly isolated nanotubes. We cut the Coulomb interaction after a distance of twice that of the diameters of BNNTs, which is necessary for both GW and BSE calculations.[43] A k-point sampling of $1 \times 1 \times 62$ is used for the single-walled BNNT (5,5) during the GW calculations, and for the BSE calculation we interpolate to 256 k-point sampling. The GW and BSE calculations are performed with YAMBO code.[44] The parameters are all converged within 0.1 eV for GW gap and absorption spectra. The parameters for BNNT (10,10) and BNNT (5,5)@(10,10) are scaled with respect to the volume according to BNNT (5,5). The convergence test of parameters can be found in the supplementary material.[50]

III. RESULTS AND DISCUSSION

Figure 1 presents the structures of three armchair BNNTs considered in this work: single-walled (5,5), (10,10) and double-walled (5,5)@(10,10). The diameters of the relaxed (5,5) and (10,10) BNNTs are 3.46 Å and 6.91 Å, respectively, and that of (5,5)@(10,10) BNNT is 3.44 Å. The choice of (5,5)@(10,10) BNNT is because the distance between the two tubes is about 3.3-3.5 Å.[28,29]

The band gaps of BNNTs increase with the increase of tube diameter, and eventually converge to the value of bulk h-BN.[45] This is because in BNNTs, σ and π states hybridize with each other as in CNTs,[46] leading to electronic structures different from those of layered BN. The single-walled (5,5) and (10,10) BNNTs are indirect semiconductors with LDA band gaps of 4.21 and 4.48 eV, respectively. When these two single-walled BNNTs are merged into the double-walled (5,5)@(10,10), the band gap decreases to 3.80 eV, smaller than both the single-walled components (shown in Figs. 2(a)–2(c)). Partial charge density analysis shows that valence band minimum (VBM) mainly originates from the outer tube, while the conduction band maximum (CBM) predominantly arises from the inner tube (Figs. 2(c) and 2(d)). The band gap decreasing in double-walled BNNT (5,5)@(10,10) is due to the downshift of π states in the outer tube smaller than that in the inner tube. However, the electronic states in the outer and inner tubes are hybridized instead of independent each other (Figs. 2(d) and 2(e)). When the double-walled BNNT is excited by light, an electron jumps from the valence band to the conduction band, e.g., from the outer tube to the inner one, leading to a hole left in the outer tube. As a result, the electron and the hole reside in the inner and the outer tubes, respectively; that is, the electron and the hole are separated and form an exciton. This type of exciton, formed from the opposite charge separation, in which the electron and hole reside in the inner and outer tubes of double-walled BNNT, respectively, is different from those in single-walled BNNTs.

The quasiparticle band gap of bulk h-BN is 1.58 eV larger than that of the LDA value.[47] But for BNNTs, the quasiparticle corrections for the indirect band gap are much larger, 2.01, 1.62, and 1.76 eV for single-walled (5,5), (10,10) and double-walled (5,5)@(10,10), respectively. We also find that for valence bands, the band stretching can be used to obtain the quasiparticle band structures, while for the conduction bands, the correction and stretching have a strong dependence on the specific band and the k points. Thus, the correct absorption spectra cannot be obtained by using simple stretching plus the scissors method. The different correction behavior stems from the existence of nearly free electron states in BNNTs (see the supplementary material[50]).

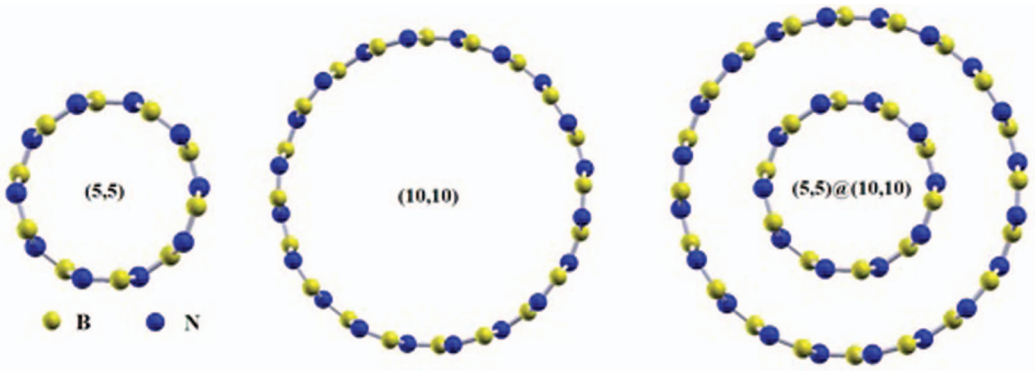

FIG. 1. Relaxed structures of armchair single-walled BNNTs (5,5), (10,10) and double-walled BNNT (5,5)@(10,10).

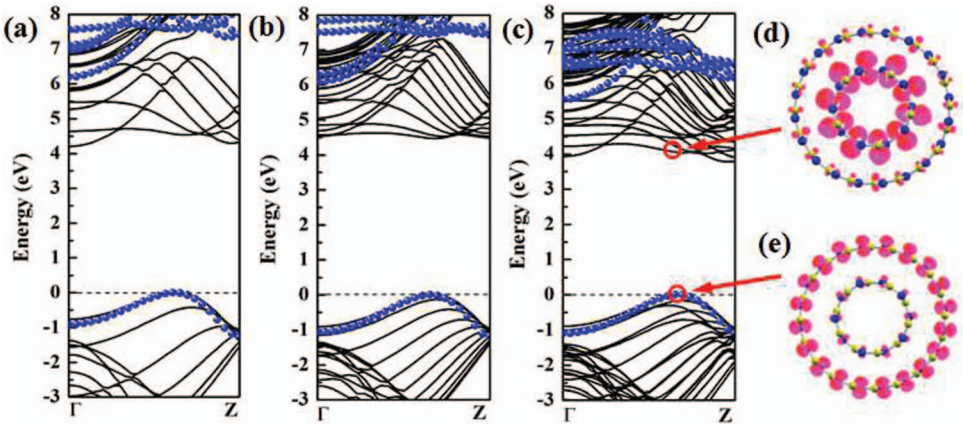

FIG. 2. Band structures of armchair single-walled BNNTs (5,5) (a), (10,10) (b), and double-walled BNNT (5,5)@(10,10) (c). The dotted lines denote the quasiparticle band. (d) and (e) are electron density of the valence band minimum and its corresponding lowest conduction band edge, respectively.

Figure 3 depicts the optical absorption spectra of (5,5), (10,10) and (5,5)@(10,10). In (5,5), the lowest-energy absorption peak is at 5.45 eV, and the corresponding exciton binding energy is 2.03 eV. This peak is also the strongest absorption one which relates to the direct transition between VBM and its corresponding conduction band edge. For (10,10), the absorption peak has a small blue-shift compared to (5,5), locating at 5.51 eV, and the exciton binding energy is 2.01 eV. In (5,5)@(10,10), the absorption lineshape loses the features of single-walled tubes accompanied with several peaks in the energy range higher than 6.0 eV (Fig. 3(c)). Similar to single-walled BNNT (5,5), the strongest absorption peak locates at 5.45 eV with an exciton binding energy of 1.95 eV. This peak correlates with the transition between the fourth valence band and the CBM, which are mainly contributed from the inner tube of BNNT (5,5)@(10,10). This indicates that interwall interaction has a minor impact on optical absorption spectra. Below the energy region of the strongest peak, there exists a series of dark or semi-dark excitons

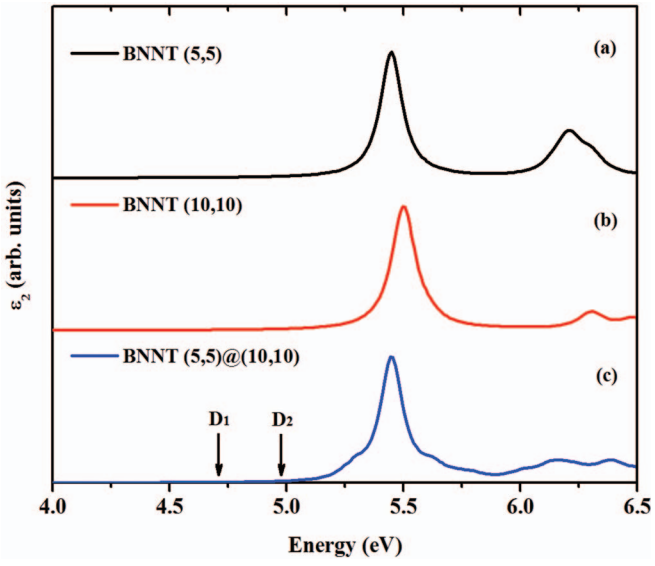

FIG. 3. Optical absorption spectra of armchair single-walled BNNTs (5,5) (a), (10,10) (b), and double-walled BNNT (5,5)@(10,10) (c) including excitonic effects. D_1 and D_2 denote the lowest 2 dark excitons.

stemming from the vertical transitions between VBM and the lowest 2 conduction band edges, which are approximately 2/3 of the way through the Brillouin zone. Arenal and coworkers[10] measured the optical absorption spectra of single and triple-walled BNNTs with the diameter range of 15-30 Å and found the optical gaps are about 5.8 ± 0.2 eV. Our results agree well with this experimental value within *GW* natural error. However, the convergence of the spectra for single BNNTs is slower than that of Wirtz *et al.*[16] In our case, the peak positions of BNNT (5,5) and BNNT (10,10) still have a 0.06 eV difference even when we used 256 *k*-point sampling, while in Ref. 16, the tube (5,5) peak converged to a constant value. According to Ref. 21, the BNNTs with smaller diameters from 2.5 to 100 nm showed a slow converging toward bulk value of PL and PLE spectra. Although optical adsorption spectra are different from PL or PLE spectra, they are expected to show a similar slow convergence to the bulk as well. In addition, in Ref. 45, the energy-loss function of single-walled BNNTs also showed a convergence process from tube diameters 3.96 Å–11.87 Å. Moreover, we think that the curvature effects would also make the absorption spectra shift since these two single tubes have a significant diameter difference of about 6.78 Å. The different convergence between ours results and Wirtz *et al.*[16] may originate from the *k*-point sampling and Coulomb cutoff since Wirtz *et al.*[16] took cutoff neither in *GW* nor in BSE calculations, which has a powerful impact on the convergence of optical absorption spectra.[43]

Real-space charge distribution of the excitons related to the strongest absorption peak in the single-walled BNNTs was shown in Fig. 4. In (5,5) BNNT (Fig. 4(a)), when the hole locates around the N atom (denoted as ×), the electron can be found around B atoms next to the hole position. The charge distribution in (10,10) (Fig. 4(b)) is analogous to that of (5,5), and there is a common feature that the charge has a symmetric distribution. This feature originates from the mirror symmetry in armchair BNNTs. In Figs. 4(b) and 4(d), along the periodic direction, the electron density symmetrically distributes at two sides of the hole, and the largest density locates at B atoms close to the hole, indicating the excitons in these two single-walled BNNTs have small diffuse areas, which are of Frenkel type. Although (5,5) and (10,10) have very different

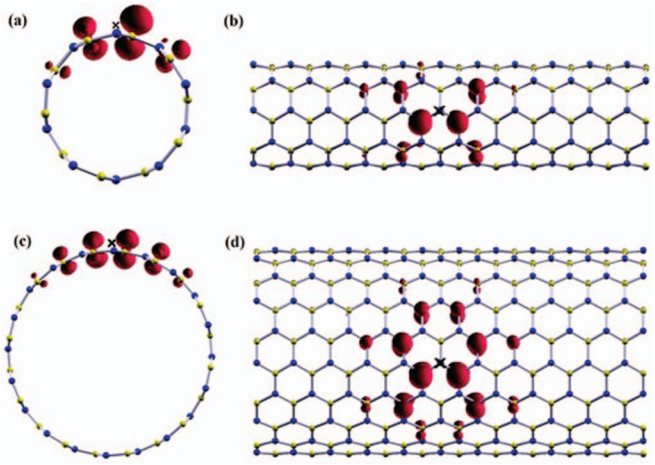

FIG. 4. Charge distribution of the excitons corresponding to the strongest absorption peak in the armchair single-walled BNNTs (5,5) (a), (b) and (10,10) (c), (d). Electron isosurface is 0.1 e/a.u.^{3}.

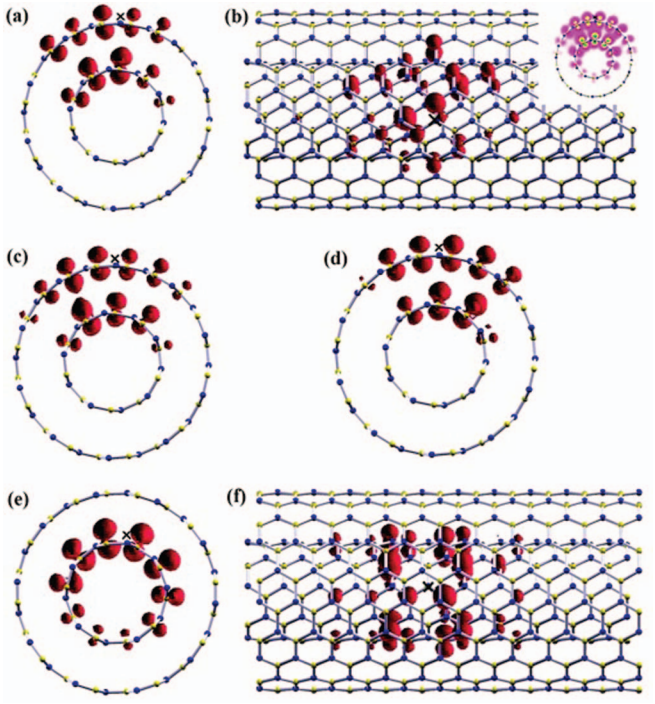

FIG. 5. Charge distribution of excitons in armchair BNNT (5,5)@(10,10): (a) (D_1 in Fig. 3(c)), (c) (D_2 in Fig. 3(c)), (d) three lowest energy excitons; (b) side view of (a); and (e), (f) the exciton related to the strongest absorption peak. Electron isosurface is 0.1 e/a.u.^{3}

diameters, their exciton charge distributions both possess fast convergence property.

Figure 5 presents the charge distribution of the three lowest energy excitons and the exciton related to the strongest absorption peak in the double-walled BNNT (5,5)@(10,10). For the case of the three lowest-energy excitons, when the hole is fixed around the N atom in the outer tube, the electron distributes over the B atoms close to the hole in the both outer and inner tubes, and the most probable distribution for the electron is in the inner tube (inset of Fig. 5(b)). The electron distribution probability in the inner and outer tubes is about 60% and 40%, respectively. We find these three excitons are dark or semi-dark resulting from the unique charge distribution in double-walled BNNT aforementioned. The excited electron can transfer from the outer tube to the inner tube,

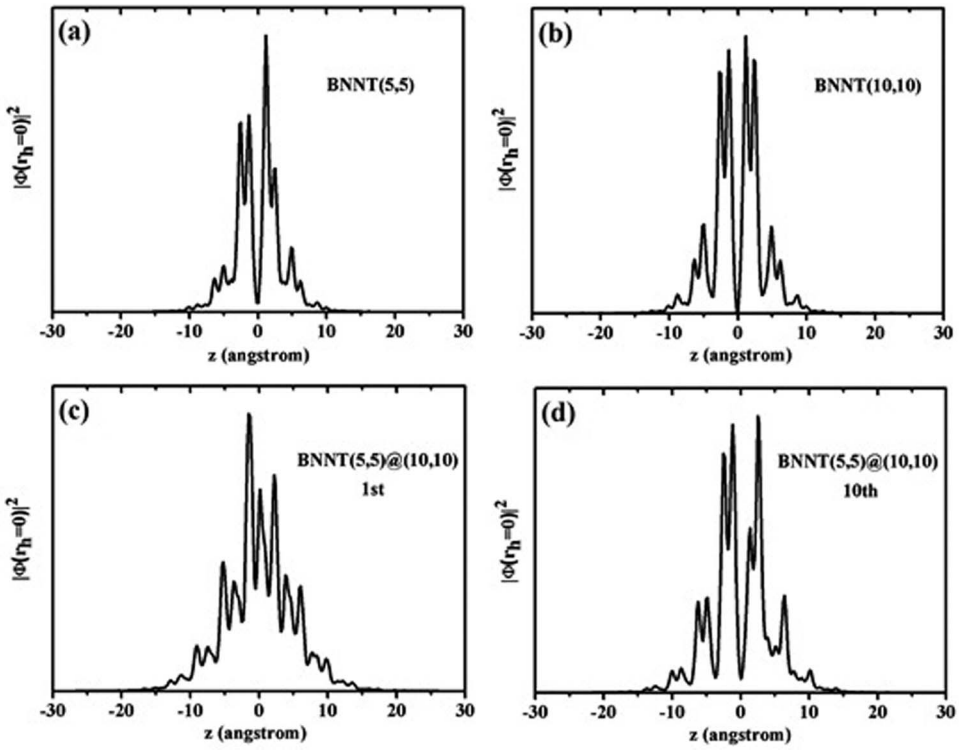

FIG. 6. Quantitative electron distribution of armchair single-walled BNNTs (a) (5,5), (b) (10,10) and double-walled BNNT (c), (d) (5,5)@(10,10). The hole fixed at z = 0. (a) and (b) correspond to the exciton with the strongest absorption peak in Figs. 3(a) and 3(b). (c) and (d) are the lowest-energy exciton and the exciton related to the strongest absorption peak in (5,5)@(10,10), respectively.

unlike that in single-walled BNNTs which can only be localized close to the hole. These charge transfer excitons lead to the further separation of the electrons and holes and lowers the recombination probability of electron-hole pairs. The fact that the electrons and holes reside at two different tubes in the double-walled BNNT, reveals that quantum confinement in double-walled tubes is weaker than that in single-walled ones. However, the story is totally different when it turns to the exciton related to the strongest absorption peak. As shown in Figs. 5(e) and 5(f), when the hole is fixed in the N atom in the inner tube, the electrons also reside at B atoms close to the hole rather than being transferred to the outer tube, which is different from that in the above-mentioned three lowest-energy excitons. This is attributed to their different transitions. For the three lowest-energy excitons, they mainly come from the transitions between the first valence band and the first or second conduction band, and these bands belong to the outer and the inner tubes, respectively, making the excited electrons transfer from one tube to another. The exciton related to the strongest absorption peak is from the transition between the fourth valence band and the first conduction band, and both of these two bands originate from the inner tube. Thus, the excited electron of this exciton can be only localized closely to the hole in the inner tube. These results indicate that in this double-walled BNNT, only the low-energy excitations cause the transference of electrons between two tubes, while the high-energy excitations still stem from one of the tubes in the double-walled BNNT. The electron transfer direction in the double-walled BNNT is inverse to that in the double-walled CNT, in which the highest valence band and the lowest conduction band root in inner and outer tubes,[32] respectively. Nevertheless, we have to point out that the double-walled BNNT considered in this work has high curvature. We can expect that similar charge-transfer excitations will be observed in a relatively broad diameter range. If the tube diameter is large enough, the double-walled tubes will be similar to the hexagonal layered structures with no curvature; therefore, the charge-transfer excitations will be rather weak and the low energy excitations will mainly be confined within one tube as reported in Refs. 48 and 49.

Quantitative pictures of the charge distribution are further displayed in Fig. 6. For (5,5) and (10,10), the expanded distance of charge in the exciton related to the strongest absorption peak is about 10 Å, indicating that the exciton distribution area has a fast convergence with the increase of the tube diameter. For (5,5)@(10,10), both of the distribution areas are 15 Å in the three lowest-energy excitons and the exciton related to the strongest absorption peak, suggesting that the outer tube has a screening effect to the inner tube, and the exciton charge expanded areas are thus wider than those in single-walled BNNTs.

IV. CONCLUSIONS

In summary, we have investigated the electronic structures and excitonic optical properties of the double-walled armchair boron nitride nanotube (5,5)@(10,10), and compared it with the single-walled boron nitride nanotubes (5,5) and (10,10). The quasiparticle energies correct the LDA direct band gap as high as 3.01 eV, more than the indirect gap correction due to the existence of the nearly free electron states. The excitonic optical absorption spectra of the double-walled nanotube hold the same position as the single-walled (5,5) one suggesting the interwall interaction is rather weak for absorption spectra. Dark and semi-dark excitons appear at a lower energy region, stemming from the electron transfer between the tubes in the double-walled structure. The electron transfer makes the excited electron and the hole reside in different tubes, and they act almost like free charges with high mobility. In addition, the electrons in BNNTs transfer from outer tubes to inner ones, which is exactly opposite to what is observed in CNTs. The screening of the outer tube also leads to the exciton binding energies in the double-walled BNNT being smaller than those of the single-walled ones. Although the insulating nature may hinder its application as a photovoltaic cell, the presence of low-lying dark excitons may lead to weak photoluminescence, and the favorable electron-hole separation may be used in UV or laser devices. Nevertheless, the screening environments can be altered via chemical decoration, applied tensile or electric field, which may induce the enhanced photoluminescence stemming from the dark-bright transfer.

ACKNOWLEDGMENTS

This work is supported by the NBRP (Grant Nos. 2011CB302004 and 2010CB923401), National Science Foundation (NSF) (Grant Nos. 21173040 and 21373045), the NSF of Jiangsu (Grant Nos. BK20130016 and BK2012322) and SRFDP (Grant No. 20130092110029) of China. The computation work was done using a computational facility at Department of Physics of Southeast University and National Supercomputing Center in Tianjin.

[1] S. Iijima, Nature (London) **354**, 56 (1991).
[2] D. Golberg, Y. Bando, W. Han, K. Kurashima, and T. Sato, Chem. Phys. Lett. **308**, 337 (1999).
[3] E. Bengu and L. D. Marks, Phys. Rev. Lett. **86**, 2385 (2001).
[4] N. G. Chopra, R. J. Luyken, K. Cherrey, V. H. Crespi, M. L. Cohen, S. G. Louie, and A. Zettl, Science **269**, 966 (1995).
[5] D. Golberg, Y. Bando, M. Eremets, K. Takemura, K. Kurashima, T. Tamiya, and H. Yusa, Appl. Phys. Lett. **69**, 2045 (1996); W. Han, Y. Bando, K. Kurashima, and T. Sato, *ibid.* **73**, 3085 (1998).
[6] A. Loiseau, F. Willaime, N. Demoncy, G. Hug, and H. Pascard, Phys. Rev. Lett. **76**, 4737 (1996); R. Arenal, X. Blase, and A. Loiseau, Adv. Phys. **59**, 101 (2010).
[7] A. Rubio, J. L. Corkill, and M. L. Cohen, Phys. Rev. B **49**, 5081(R) (1994).
[8] X. Blase, A. Rubio, S. G. Louie, and M. L. Cohen, Europhys. Lett. **28**, 335 (1994).
[9] J. S. Lauret, R. Arenal, F. Ducastelle, A. Loiseau, M. Cau, B. Attal-Tretout, E. Rosencher, and L. Goux-Capes, Phys. Rev. Lett. **94**, 037405 (2005).
[10] R. Arenal, O. Stéphan, M. Kociak, D. Taverna, A. Loiseau, and C. Colliex, Phys. Rev. Lett. **95**, 127601 (2005).
[11] T. Ando, J. Phys. Soc. Jpn. **66**, 1066 (1997).
[12] C. D. Spataru, S. Ismail-Beigi, L. X. Benedict, and S. G. Louie, Phys. Rev. Lett. **92**, 077402 (2004).
[13] F. Wang, G. Dukovic, L. E. Brus, and T. F. Heinz, Science **308**, 838 (2005).
[14] Y.-Z. Ma, L. Valkunas, S. L. Dexheimer, S. M. Bachilo, and G. R. Fleming, Phys. Rev. Lett. **94**, 157402 (2005).
[15] Y.-Z. Ma, L. Valkunas, S. M. Bachilo, and G. R. Fleming, J. Phys. Chem. B **109**, 15671 (2005).
[16] L. Wirtz, A. Marini, and A. Rubio, Phys. Rev. Lett. **96**, 126104 (2006).

[17]C.-H. Park, C. D. Spataru, and S. G. Louie, Phys. Rev. Lett. **96**, 126105 (2006).
[18]B. Berzina, L. Trinkler, V. Korsak, R. Krutohvostov, D. L. Carroll, K. B. Ucer, and R. T. Williams, Phys. Status Solidi B **243**, 3840 (2006).
[19]H. Chen, Y. Chen, Y. Liu, C.-N. Xu, and J. S. Williams, Opt. Mater. **29**, 1295 (2007).
[20]P. Jaffrennou, J. Barjon, T. Schmid, L. Museur, A. Kanaev, J.-S. Lauret, C. Y. Zhi, C. Tang, Y. Bando, D. Golberg, B. Attal-Trétout, F. Ducastelle, and A. Loiseau, Phys. Rev. B **77**, 235422 (2008).
[21]J. Yu, D. Yu, Y. Chen, H. Chen, M.-Y. Lin, B.-M. Cheng, J. Li, and W. Duan, Chem. Phys. Lett. **476**, 240 (2009).
[22]G. Brasse, S. Maine, A. Pierret, P. Jaffrennou, B. Attal-Trétout, F. Ducastelle, and A. Loiseau, Phys. Status Solidi B **247**, 3076 (2010).
[23]M. Radosavljević, J. Appenzeller, V. Derycke, R. Martel, Ph. Avouris, A. Loiseau, J.-L. Cochon, and D. Pigache, Appl. Phys. Lett. **82**, 4131 (2003).
[24]K. Watanabe, T. Taniguchi, and H. Kanda, Nat. Mater. **3**, 404 (2004).
[25]C. Y. Zhi, Y. Bando, C. C. Tang, D. Golberg, R. Xie, and T. Sekiguchi, Appl. Phys. Lett. **86**, 213110 (2005).
[26]D. Golberg, Y. Bando, K. Kurashima, and T. Sato, Solid State Commun. **116**, 1 (2000).
[27]A. Zettl, *Abstracts of the Tsukuba Symposium on Carbon Nanotubes in Commemoration of the 10th Anniversary of Its Discovery* (Science Academy Tsukuba, Tsukuba, 2001), p. 10.
[28]S. Okada, S. Saito, and A. Oshiyama, Phys. Rev. B **65**, 165410 (2002).
[29]D. Golberg, Y. Bando, Y. Huang, T. Terao, M. Mitome, C. Tang, and C. Zhi, ACS Nano **4**, 2979 (2010).
[30]S.-H. Jhi, D. J. Roundy, S. G. Louie, and M. L. Cohen, Solid State Commun. **134**, 397 (2005).
[31]H. Hirori, K. Matsuda, and Y. Kanemitsu, Phys. Rev. B **78**, 113409 (2008).
[32]T. Koyama, Y. Asada, N. Hikosaka, Y. Miyata, H. Shinohara, and A. Nakamura, ACS Nano **5**, 5881 (2011).
[33]A. A. Green and M. C. Hersam, ACS Nano **5**, 1459 (2011).
[34]P. Jaffrennou, J. Barjon, J.-S. Lauret, A. Maguer, D. Golberg, B. Attal-Trétout, F. Ducastelle, and A. Loiseau, Phys. Status Solidi B **244**, 4147 (2007).
[35]G. Onida, L. Reining, and A. Rubio, Rev. Mod. Phys. **74**, 601 (2002).
[36]P. Giannozzi, S. Baroni, N. Bonini *et al.*, J. Phys.: Condens. Matter **21**, 395502 (2009).
[37]M. S. Hybertsen and S. G. Louie, Phys. Rev. B **34**, 5390 (1986).
[38]L. Hedin, Phys. Rev. **139**, A796 (1965).
[39]W. von der Linden and P. Horsch, Phys. Rev. B **37**, 8351 (1988).
[40]G. E. Engel and B. Farid, Phys. Rev. B **47**, 15931 (1993).
[41]M. Rohlfing and S. G. Louie, Phys. Rev. B **62**, 4927 (2000).
[42]G. Strinati, Phys. Rev. B **29**, 5718 (1984).
[43]C. A. Rozzi, D. Varsano, A. Marini, E. K. U. Gross, and A. Rubio, Phys. Rev. B **73**, 205119 (2006).
[44]A. Marini, C. Hogan, M. Grüning, and D. Varsano, Comput. Phys. Commun. **180**, 1392 (2009).
[45]G. Y. Guo and J. C. Lin, Phys. Rev. B **71**, 165402 (2005).
[46]X. Blase, L. X. Benedict, E. L. Shirley, and S. G. Louie, Phys. Rev. Lett. **72**, 1878 (1994).
[47]X. Blase, A. Rubio, S. G. Louie, and M. L. Cohen, Phys. Rev. B **51**, 6868 (1995).
[48]B. Arnaud, S. Lebègue, P. Rabiller, and M. Alouani, Phys. Rev. Lett. **96**, 026402 (2006).
[49]M. Ashhadi and S. A. Ketabi, Solid State Commun. **187**, 1 (2014).
[50]See supplementary material at http://dx.doi.org/10.1063/1.4880726 for convergence test results and quasiparticle corrections versus LDA energies of BNNTs.